

Power Law Averaging Revisited

Stefan Zanon (zanon@ualberta.ca), Hanh Nguyen (hanh_nguyen@gulf.ca)
and Clayton V. Deutsch (cdeutsch@ualberta.ca)

Department of Civil & Environmental Engineering, University of Alberta

Abstract

Power law averaging was developed to scale up fine grid permeability models to effective permeability models on a coarse grid for flow simulation. Direct calculation of effective permeability with selected boundary conditions has largely replaced the need for heuristic scaling procedures such as power law averaging. Nevertheless, new areas of application have emerged for power law averaging. First, successful integration of well test and production data requires techniques to simultaneously account for small scale data, coming from core and log measurements, with large scale data coming from well test and production data. The power law formalism can be used to transform the various permeability data so that the transformed values average linearly, which is a requirement of geostatistical techniques. Second, the effective permeability in sandstone/shale systems can be calculated with the volume fraction of shale and the constituent permeability values, provided that the directional averaging exponents can be calibrated to the geological setting. The theory behind power law averaging is revisited and new areas of application are developed.

The Use of Power Law in Modern Geostats

Power law averaging was developed to upscale fine scale realizations to coarse scale models for flow simulation (Deutsch, 1989); however, with increases in computing power, upscaling is easily performed with quick flow simulators instead of approximative scaling relations (Durlafsky, 1990 and many other references). We will revisit power law averaging and describe possible applications in modern reservoir characterization.

Among other things, well log data provide a measure of porosity and the volume fraction of shale. The porosity data can be used directly, but when permeability measurements are sparse, permeability must be based on the combined spacial characteristics of the shale and sandstone. The power law averaging method provides a way to calculate directional permeability values that account for the orientation of the shales. Figure 1 shows schematically how the V_{shale} log data can be transformed to a range of horizontal and vertical permeabilities based on different ω values in the power law transformation.

Another problem in modern geostatistics is the integration of small scale core-based permeability with large-scale production data. See Figure 2 for a schematic illustration of the different scales at which data is collected and how they are combined to create multiple realizations at an intermediate scale. The problem is the vast difference in scale and the highly non-linear averaging of permeability. To further complicate this situation, modelling is often performed at an intermediate scale between the core and production data. Gaussian techniques require the data to be transformed to a Gaussian distribution, but permeability does not average linearly after Gaussian transformation; however, a power law transform of permeability provides values that average linearly and permits the data to be simultaneously accounted for in modelling via a direct simulation approach.

When unstructured grids are used the data must be linear with scale and power law averaging provides a means to do this. Figure 3 shows an example of an unstructured grid with cells that vary in size. Modern flow simulators are tending towards unstructured grids. Power law transformation will permit direct modelling of different volumes with block kriging.

This paper starts with a review of power law averaging and why it is important. We then explain how it is implemented. This is followed with a discussion of implementation issues and examples.

Background

The general formula for power law averaging of the continuous variable K is written:

$$K_{eff} = \left[\frac{1}{v} \int_v k(\mathbf{u})^\omega d\mathbf{u} \right]^{\frac{1}{\omega}} \quad (1)$$

v is the volume over which the average is calculated, $k(\mathbf{u})$ is the permeability at location \mathbf{u} within the volume, and ω is an exponent of averaging.

The averaging for the categorical case is written:

$$K_{eff} = \left(\sum_{i=1}^{i=n} p_i K_i^\omega \right)^{\frac{1}{\omega}} \quad (2)$$

Where n is the number of classes, p_i is the volume fraction of class i , and K_i is the permeability of class i . For a binary system of sandstone/shale, the power average equation is written:

$$K_{eff} = [V_{sh} K_{sh}^\omega + (1 - V_{sh}) K_{ss}^\omega]^{\frac{1}{\omega}} \quad (3)$$

Where K_{sh} is the permeability of shale, K_{ss} is the permeability of sandstone and V_{sh} is the volume fraction of shale.

The effective permeability, K_{eff} , of a 3-D network of blocks must take a value between the harmonic and arithmetic average of the constituent permeabilities, depending on their spatial arrangement. The lower-bound harmonic average can be seen as a power average with $\omega = -1$; this is representative of flowing through a series of alternating permeability layers. The upper-bound arithmetic average can be seen as a power average with $\omega = +1$; this represents parallel flow through alternating permeability layers. The geometric average is obtained at the limit when $\omega = 0$. A proof of the geometric average as $\omega \rightarrow 0$ can be found in Appendix A.

The problem of determining the effective permeability can be transferred to the problem of determining the constituent permeabilities and the averaging power.

Effective permeability is sensitive to the underlying spatial structure of the permeability values and the averaging process. Consider a reservoir volume with 50% good quality reservoir rock at 100 mD and 50% poor quality rock at 0.01 mD. The average permeability can take any value between 0.02 mD and 50 mD, depending on the spatial continuity of the different permeability rock and the direction of flow. The calculated effective permeability can differ by many orders of magnitude depending on the averaging process. An incorrect assumption about the spatial structure could lead to significant errors.

An important observation is that the averaging exponents in the principal directions depend on the spatial continuity and the geological setting but not on the univariate histogram or the amount of good/poor quality reservoir rock. This observation makes power-law averaging useful.

Methodology

Kriging-based geostatistical techniques require variables that average linearly with scale. Permeability in its original units or after Gaussian transformation does not average linearly. This causes problems with data at different scales and when using a different modeling scale. This problem can be avoided by using a power law transformation; the transformed values average linearly with scale.

The challenge is to determine the direction-dependent exponents, ω_X , ω_Y and ω_Z . The ω values are between the arithmetic and harmonic averages, or 1.0 and -1.0. The exponents depend mostly on the spatial features in the formation and not the histogram of the data. When flow is parallel to layering the effective permeability will be closer to the arithmetic average of constituent permeabilities. The effective permeability perpendicular to the layering will be closer to the harmonic average. In practice, ω will be somewhere between these two extreme cases.

A power law transformation does not change the basic geostatistical modelling process. A first step is to obtain ω for the principal directions. This is done by creating multiple realizations of the geological model and solving for the directional ω values. Alternatively, a collection of models could be studied and used as template for different geological situations. In this case the template with the closest geological structure could be used for the directional ω values. Once the ω values have been determined, the data of all types and volume supports can be transformed into power law space: one transform per direction. After the transformation, the histogram and variogram are determined. These statistics and the transformed data are then used for modelling using a direct simulation technique (Xu and Journel, 1994).

There may be a need to transform log-derived volume fraction of shale *Vsh* data to directional permeability values, see Figure 1. Power-law averaging could be used to provide a continuous estimate of the permeability in the horizontal and vertical directions. To start, ω values need to be calculated by modelling or using a template. These ω values are used to transform the *Vsh* data into permeability by using the binary power law formula, Equation 3. There is uncertainty in the resulting effective permeability values due to uncertainty in the power law exponent; the log data do not directly measure permeability. To account for this uncertainty, multiple ω values, that cover the full distribution of possible ω values, can be used in the transformation process. This will provide a distribution of possible K values at each location.

Calibration

The calibration process for a single geological model is straightforward. The numerical model of small scale permeabilities is subjected to flow simulation with specified boundary conditions to obtain the true effective permeabilities: K_X , K_Y , and K_Z . Average permeability values can also be calculated from the small scale permeabilities for any ω . This allows us to choose the ω_X , and ω_Y and ω_Z .

To account for uncertainty and ergodic fluctuations in the geological models we must repeat the calibration process for multiple realizations of the same geological model. Once an assemblage of directional ω values have been calculated, the resulting distributions can be checked. The mean value will provide a single estimate for ω in a given direction, and the distribution will show the uncertainty in ω for the geological model.

The `flowsim` program (Deutsch, 1987) can be used to solve for the directional effective permeability values given a geological model. Appendix B describes a program to calibrate ω based on the effective permeabilities and the small scale permeability values. The ω value is calculated in four steps: (1) construct multiple permeability realizations based on a specific geological model, (2) calculate the effective K_X , K_Y , and K_Z values by flow simulations, (3) calculate the directional ω values based on the flow simulation results and the original realizations, and (4) plot a histogram of the resulting directional ω values.

Implementation Issues

An ω derived from a synthetic geological model will have uncertainty. Multiple realizations of the same geological model provides one way to assess this uncertainty. The resulting distribution of directional ω represents the range of possible ω values for that model. For practical purposes the mean can be used for a single best estimate and uncertainty can be estimated by using upper and lower percentiles, say the 10th and 90th. Alternatively we could use Monte Carlo simulation from the ω distribution and the resulting uncertainty can then be quantified. This uncertainty can be carried through the rest of the modelling process.

Models based on different geological structures could be considered. For example, elliptical remnant shales and shales created by overlapping fluvial sands. The results of different geological models can be compared and appropriate uncertainty transferred through subsequent steps.

In calculating the effective permeability in a binary situation, Equation 3, we require the permeabilities for the constituent shale and sandstone. The sandstone permeability can be calculated from core plugs and a distribution of different values could be considered; however, the shale permeabilities are often more difficult to obtain. Shale permeabilities can range from 0.01 to 0.000001 mD, which can affect the calculated effective permeability values. The affect of this uncertainty is minimized by using the same K_{sh} values in the calibration and calculation step.

Another problem with binary systems is that once a critical percentage of shale has been exceeded, all the flow paths must go through shale. This causes a dramatic change in the effective permeability since we can no longer flow through sandstone. In trying to work with a histogram near this percolation threshold, about 80% in a 3 dimensional correlated model, care must be taken to calibrate the model separately for shale fractions above and below this threshold.

A final concern is that ω may not be constant over every volume support. Large changes in volume will likely cause the ω value to change. This complicates calibration.

Examples

Multiple `sgsim` realizations (Deutsch and Journel, 1997) were created for anisotropy ratios ranging from 1:1 to 25:1. A lognormal distribution of permeability was considered. These realizations were flow simulated and the ω values calibrated. Figure 4 shows the histograms for each direction and anisotropy ratio. As the anisotropy ratio increases the direction perpendicular to the greatest continuity will see a decrease in ω ; the 2 directions parallel to the continuity will see an increase in ω . Figure 5 shows these results in a graphical format where the black dots are the average for each distribution and the red and blue lines represent one deviation above and below. The variance of ω is small, being the highest at the low anisotropy ratio and decreasing as this ratio increases. Note

that a 2-D example with anisotropy ratio of 1 should yield an ω of zero (Matheron, 1969), but in 3-D the ω will be higher at about 0.2.

Next, ellipsoidal shale intrusions within a sandstone matrix were created, using `ellipsim` (Deutsch and Journel, 1997). Two studies were performed. One study looked at the effects of changing the anisotropy ratio and the other showed the effects of changing the shale percentage. 51 realizations of 125,000 1.0m blocks were created for each study. The histograms for the anisotropy study are shown in Figure 6. Once again, as the anisotropy ratio increases the ω value decreases for flow perpendicular to continuity and increases in the directions parallel to continuity. Figure 7 shows the mean and variance as before, but in this case the variance increases as the anisotropy ratio increases. The percentage study showed only a small change in ω as the percentage changed from 5% to 65% shale. The histograms are seen in Figures 8 and 9 with the mean and variance values shown in Figure 10. These results show little variability in ω for each anisotropy ratio, but Figure 10 indicates that as the anisotropy ratio goes to infinity the ω values approach a single value. An upper limit of 65% was used to avoid the percolation threshold. These studies show that the ω is mostly dependent on the spatial parameters and not the histogram.

`ellipsim` is an object based modelling program that randomly places 3-D ellipsoids in a host matrix. The size of the ellipsoids is defined by the user. Different anisotropy ratios are considered by varying the size of the radii of the ellipsoids.

A final study looked at how ω changes in a fluvial setting using the `fluvsim` program (Deutsch and Tran, 1997). 51 realizations were created for 3 different scenarios. A base case scenario was chosen, see Figure 11. A “thick” case was used where the width was halved and the depth was doubled, see Figure 12. A “thin” case was also considered where the width was doubled and the thickness halved, see Figure 13. Each figure shows the histograms for ω and three vertical and horizontal cross sections. ω is more variable in this setting than in previous examples, especially perpendicular to the fluvial channels.

The `fluvsim` program is an object based simulation program that creates channel intrusions into a host rock. The channel cross section is similar to a half ellipsoid, but the shape will change as the channel meanders through the rock. The shape of the channels are based on parameters such as thickness and width. The program creates realizations by starting with a model of floodplain shale and then embedding channels with parameters drawn from the distributions. This process continues until a target proportion of channels has been created.

A set of Vsh log data, Figure 14, was transformed to effective permeabilities using the directional ω values from the base `fluvsim` case. The transformation was performed in three directions using the mean, 10th percentile, and 90th percentile ω values. In the X direction (across channel flow) the effective permeability shows some variability depending on the value of ω_X , see Figure 15. The thick black line shows the results for the mean ω_X value and the blue and red lines represent the P_{10} and P_{90} ω_X values, respectively. The Y direction (parallel to channel flow) shows almost no variability since ω_Y is very consistent in this direction, see Figure 16. Finally, in the Z direction (vertically) ω_Z has a large degree of variability and this transfers to uncertainty in the effective permeability in this direction, see Figure 17.

Another way to look at these results is to consider the permeability ratios between the directions, see Figure 18. The upper two left plots show k_x/k_y ratios (red) and k_z/k_y ratios (blue) in arithmetic and log scales. The lower left two plots show the same ratios with different values for K_{sh} . The red, black, and blue lines represent K_{sh} values of 1.0, 0.001, and 0.000001 mD respectively. The right four plots is the original Vsh data for comparison. To better understand how the permeability

ratios are affected by Vsh , Figure 19 was created. The top plot looks at the K_X/K_Y , in arithmetic units, versus Vsh . The points are from the example Vsh data set and the solid line is from a synthetic data set which was created to cover the full range of Vsh values. The lower plot looks at the K_Z/K_Y , in logarithmic units, versus the Vsh percentage.

A final look at how the histogram affects ω was done using different means and standard deviations values in the lognormal transformation. Figure 20 shows the resulting directional ω distributions for a mean of 10 and standard deviations of 1, 10, and 100. Figure 21 is for a mean of 1 and the same standard deviations. Figure 22 shows the histograms of the log normal data with a mean of 10 and standard deviations of 100, 10, and 1 respectively from top down. The three vertical lines show the harmonic (blue), geometric (black), and arithmetic (red) permeabilities. As the variance decreases and the distribution approaches the mean value, the three base cases for the permeabilities approach the mean or arithmetic average.

Conclusions

Power law averaging has been around for many years but recently it has found new applications in the petroleum industry. In dealing with volume dependent variables that scale non-linearly, a power law transformation can be used to transform the variables to scale linearly. These variables can then be used for modelling, independent of their volume support, by using a direct sequential simulation formalism. The resulting realizations are then back transformed to original units for further post processing.

The power law technique has been shown to work well for several applications where the value must average linearly. There are some assumptions made in the calibration process that may effect ω . Arbitrary boundary conditions affect the calibrated ω values. Also, if the formation approaches the percolation threshold, the ω value will change. The ω might also change with vastly different scales, particularly as the nature of the geological correlation changes.

References

1. Deutsch, C. "Calculating effective absolute permeability in sandstone/shale sequences," SPE Formation Evaluation, September 1989.
2. Journel, A. Deutsch, C. and Desbarats, A. "Power averaging for block effective permeability," SPE paper 15128, 1986.
3. Deutsch, C. and Journel, A. "GSLIB: Geostatistical software library and user's guide," Oxford University Press, 1998.
4. Desbarats, A. J. "Numerical estimation of effective permeability in sand-shale formations," Water Resources Research, 23; 2, P273-286, 1987.
5. Matthews, M. D. and Zeitlin M. J. "The importance of quantitative stratigraphic modeling to basin modeling," AAPG Annual Convention, 1997.
6. Matheron, G. "Change of support for diffusion-type random functions," IAMG, 17; 2, P137-165, 1985.

7. Bachu, S. and Cuthiell, D. "Effects of Core-Scale Heterogeneity on Steady State and Transient Fluid Flow in Porous Media: Numerical Analysis," *Water Resources Research*, 26; 5, P863-874, 1990.
8. Cuthiell, D. L. Bachu, S. Kramers, J. W. and Yuan, L. P. "Characterizing shale clast heterogeneities and their effect on fluid flow," *Second International Symposium on Reservoir Heterogeneities*, 1989.
9. Desbarats, A. J. "Stochastic Modeling of Flow in Sand-Shale Sequences," *Stanford University*, 1987.
10. Desbarats, A. J. and Srivastava, R. M. "Geostatistical Characterization of Groundwater Flow Parameters in a Simulated Aquifer," *Water Resources Research*, 27; 5, P687-698, 1991.
11. Durlofsky, L. J. "Modeling Fluid Flow Through Complex Reservoir Beddings," *SPE*, 1991.
12. Durlofsky L.J. "Numerical Calculation of equivalent Grid Block Permeability Tensors for Heterogeneous Porous Media," *Water Resources Research*, 27; 5, P699-708, 1991.

Appendix A

The arithmetic, geometric, and harmonic averages are well known:

$$K_A = \frac{1}{n} \sum_{i=1}^n K_i, \quad K_G = \frac{1}{n} \prod_{i=1}^n K_i, \quad \text{and} \quad K_H = \left[\frac{1}{n} \sum_{i=1}^n \frac{1}{K_i} \right]^{-1} \quad (4)$$

where n is the number of permeability values: $K_i, i = 1, \dots, n$. These averaging cases are generalized by power-law averaging:

$$K_\omega = \left[\frac{1}{n} \sum_{i=1}^n K_i^\omega \right]^{\frac{1}{\omega}} \quad (5)$$

where the exponent ω is 1, 0, and -1 for the arithmetic, geometric, and harmonic averages, respectively.

The geometric average K_G is obtained with $\omega = 0$ at the limit. For fun, let's show a proof. Take the log of both sides of equation 5 and pull ω out

$$\ln(K_{eff}) = \left(\frac{1}{\omega}\right) \left(\frac{1}{n} \sum_{i=1}^n \omega \ln(K_i)\right)$$

rearrange to

$$\ln(K_{eff}) = \frac{\omega \sum_{i=1}^n \frac{\ln(K_i)}{n}}{\omega}$$

We want the limit as $\omega \rightarrow 0$. Recall L'Hospital's rule.

$$\lim_{x \rightarrow b} \frac{f(x)}{g(x)} = \lim_{x \rightarrow b} \frac{f'(x)}{g'(x)}$$

Define $x = \omega$ and

$$f(\omega) = \omega \sum_{i=1}^n \frac{\ln(K_i)}{n} \rightarrow f'(\omega) = \sum_{i=1}^n \frac{\ln(K_i)}{n}$$

$$g(\omega) = \omega \rightarrow g'(\omega) = 1$$

Substituting into L'Hospital's rule:

$$\ln(K_{eff}) = \lim_{x \rightarrow b} \frac{f(x)}{g(x)} = \lim_{x \rightarrow b} \frac{f'(x)}{g'(x)} = \sum_{i=1}^n \frac{\ln(K_i)}{n}$$

This now satisfies L'Hospital's rule and we have cancelled out all of the ω in the formula.

$$\ln(K_{eff}) = \frac{1}{n} \sum_{i=1}^n \ln(K_i)$$

We now raise both sides by the Euler number (e). This cancels the natural log on the left hand side.

$$e^{\ln(K_{eff})} = e^{\frac{1}{n} \sum_{i=1}^n \ln(K_i)} = K_{eff}$$

$$e^{\sum_{i=1}^n \ln(K_i)} = e^{\ln(K_1) + \ln(K_2) + \ln(K_3) \dots} = e^{\ln(K_1)} * e^{\ln(K_2)} * e^{\ln(K_3)} \dots$$

$$e^{\ln(K_1)} * e^{\ln(K_2)} * e^{\ln(K_3)} \dots = K_1 * K_2 * K_3 \dots = \prod_{i=1}^n K_i$$

$$K_{eff} = \left(\frac{1}{n} \prod_{i=1}^n K_i \right) = K_G$$

Appendix B

This section shows the parameter files for the two programs written for this project. The `calibw` program is used to calibrate ω from the original data and the quick flow results. The `wlog` program is used to transform vshale log data to an effective permeability based on a power law transform.

Parameters for Calibw

START OF PARAMETERS

calibw.out	-file for calibw output
sgsim.out	-file with small scale perm
flowsim.out	-file with flowsim output
51	-number of realizations
50 50 50	-size of grid (nx,ny, and nz)
100	-number of iterations

Parameters for WLOG

START OF PARAMETERS:

vshdata.dat	-file with log Vshale data
1 3	-Depth data and Vshale data columns
wlog.out	-output data file
0.50 0.25 0.75	-Wx mean, Wx Q10, Wx Q90
0.50 0.25 0.75	-Wy mean, Wy Q10, Wy Q90
0.15 0.05 0.25	-Wv mean, Wv Q10, Wv Q90
0.001 1000	-K Shale md, K Sandstone md
0	- 0 for K output or 1 for K Ratios

The next sample code is an example of the scripted used to find the directional ω distributions. This shows the calculation of ω for the Ellipsim program at 5% shale.

```

# Build Ellipsim Realizations P = 0.05
cat<<END>temp
START OF PARAMETERS:
ellipsim.out          -file for output realizations
51                    -number of realizations
50  0.  1.0           -nx,xmn,xsiz
50  0.  1.0           -ny,ymn,ysiz
50  0.  1.0           -nz,zmn,zsiz
69069                 -random number seed
0.05                  -target proportion (in ellipsoids)
5.0 5.0 0.5 0.0 0.0 0.0 1.0
END
ellipsim temp

# Covert Rock type to mD value (100 for sandstone, 0.001 for shale)
sed -e "s/^1/\ 0\0.001/g" -e "s/^0/100\0.0/g" ellipsim.out > temp
mv temp ellipsim.out

#Flowsim The realizations
cat<<END>temp
START OF PARAMETERS
ellipsim.out          \Input datafile with
1  0  0  0  0         \columns for kx,ky,kz, ky/kx, kz/kx
flowsim.out           \output file for effective permeabilities
  51                  \number of realizations
  50      50      50   \input : nx, ny, nz
1.0      1.0      1.0  \input : dx, dy, dz
  1      1      1     \output: nx, ny, nz
END
flowsim<<END
temp
END

#Calibrate for W
cat<<END>temp
START OF PARAMETERS
calibw-P-05.out       -file for calibw output
ellipsim.out          -file with small scale perm
flowsim.out           -file with flowsim output

```

```

51                -number of realizations
50 50 50          -size of grid (nx,ny, and nz)
100              -number of iterations
END

calibw temp

# Remove files no longer needed
rm ellipsim.out flowsim.out

# Hist Plot the 'w' variables
#For X Direction
cat<<END>temp
START OF PARAMETERS:
calibw-P-05.out   -file with data
3 0              - columns for variable and weight
-20 20           - trimming limits
hist-wX-P-05.ps   -file for PostScript output
-1.0 1.0         -attribute minimum and maximum
-1.0             -frequency maximum (<0 for automatic)
40              -number of classes
0               -0=arithmetic, 1=log scaling
0               -0=frequency, 1=cumulative histogram
0               - number of cum. quantiles (<0 for all)
3               -number of decimal places (<0 for auto.)
wX Hist (P-05)
1.5             -positioning of stats (L to R: -1 to 1)
-1.1e21         -reference value for box plot
END

histplt temp

#For Y Direction
cat<<END>temp
START OF PARAMETERS:
calibw-P-05.out   -file with data
5 0              - columns for variable and weight
-20 20           - trimming limits

```

```

hist-wY-P-05.ps          -file for PostScript output
-1.0  1.0               -attribute minimum and maximum
-1.0                    -frequency maximum (<0 for automatic)
40                      -number of classes
0                      -0=arithmetic, 1=log scaling
0                      -0=frequency, 1=cumulative histogram
0                      - number of cum. quantiles (<0 for all)
3                      -number of decimal places (<0 for auto.)
wY Hist (P-05)
1.5                    -positioning of stats (L to R: -1 to 1)
-1.1e21                -reference value for box plot
END

```

```
histplt temp
```

```
#For Z Direction
```

```
cat<<END>>temp
```

```
START OF PARAMETERS:
```

```
calibw-P-05.out
```

```
7  0
```

```
-20  20
```

```
hist-wZ-P-05.ps
```

```
-1.0  1.0
```

```
-1.0
```

```
40
```

```
0
```

```
0
```

```
0
```

```
3
```

```
wZ Hist (P-05)
```

```
1.5
```

```
-1.1e21
```

```
END
```

```
histplt temp
```

```
rm temp
```

```
histplt temp
```

```

- file with data
- columns for variable and weight
- trimming limits
- file for PostScript output
- attribute minimum and maximum
- frequency maximum (<0 for automatic)
- number of classes
-0=arithmetic, 1=log scaling
-0=frequency, 1=cumulative histogram
- number of cum. quantiles (<0 for all)
- number of decimal places (<0 for auto.)
- positioning of stats (L to R: -1 to 1)
- reference value for box plot

```

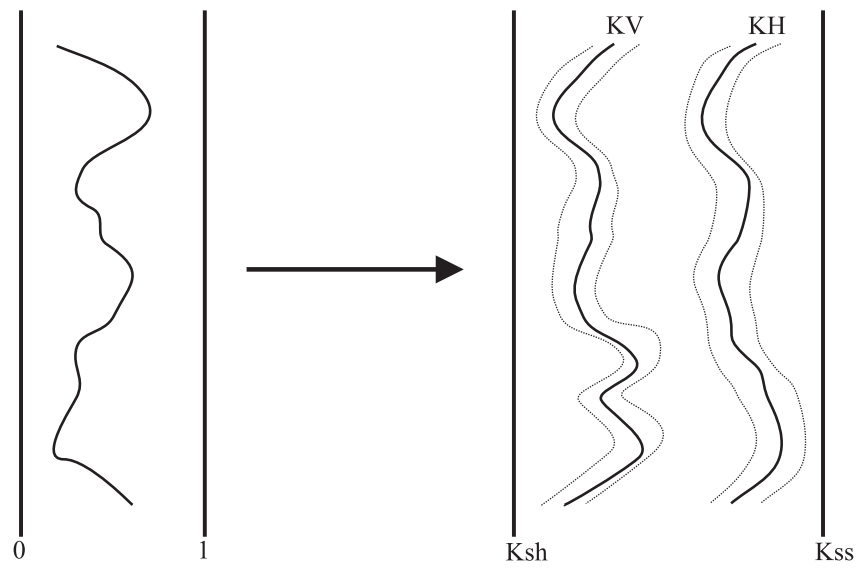


Figure 1: Power law averaging is used to transform log data into effective permeabilities.

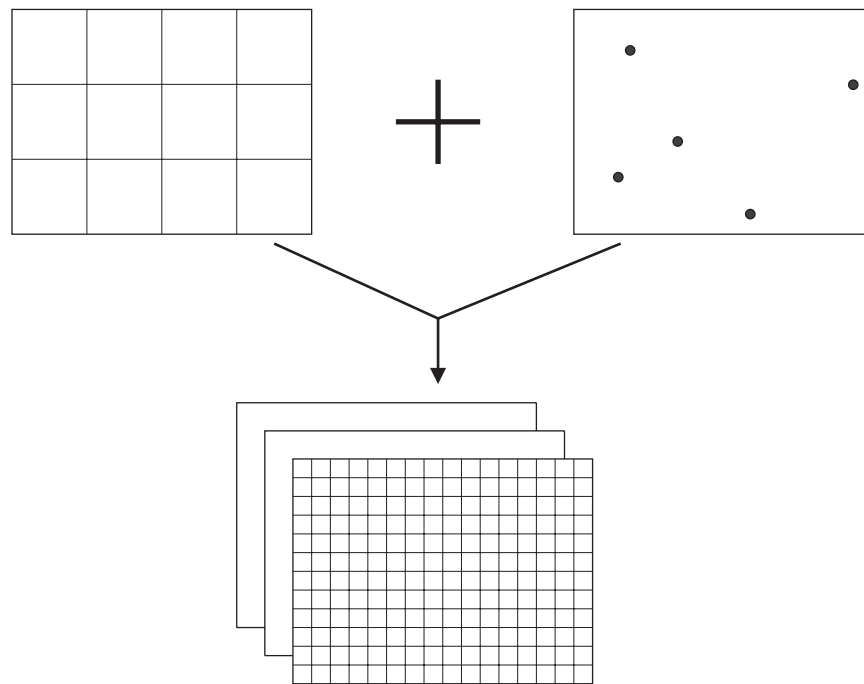


Figure 2: Integration data from different size scales can use power law averaging to create a linear relation with scale.

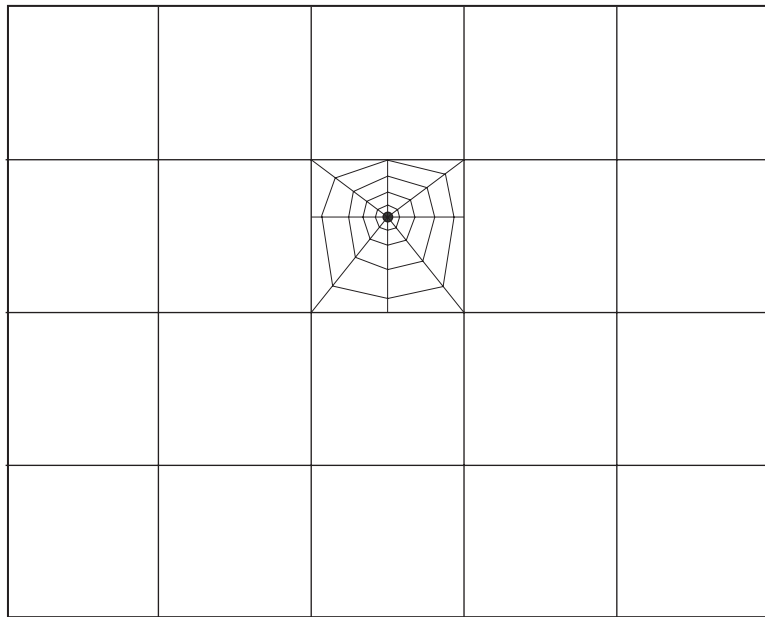


Figure 3: Power law averaging is used to linearly scale the data to any grid size when using unstructured grids.

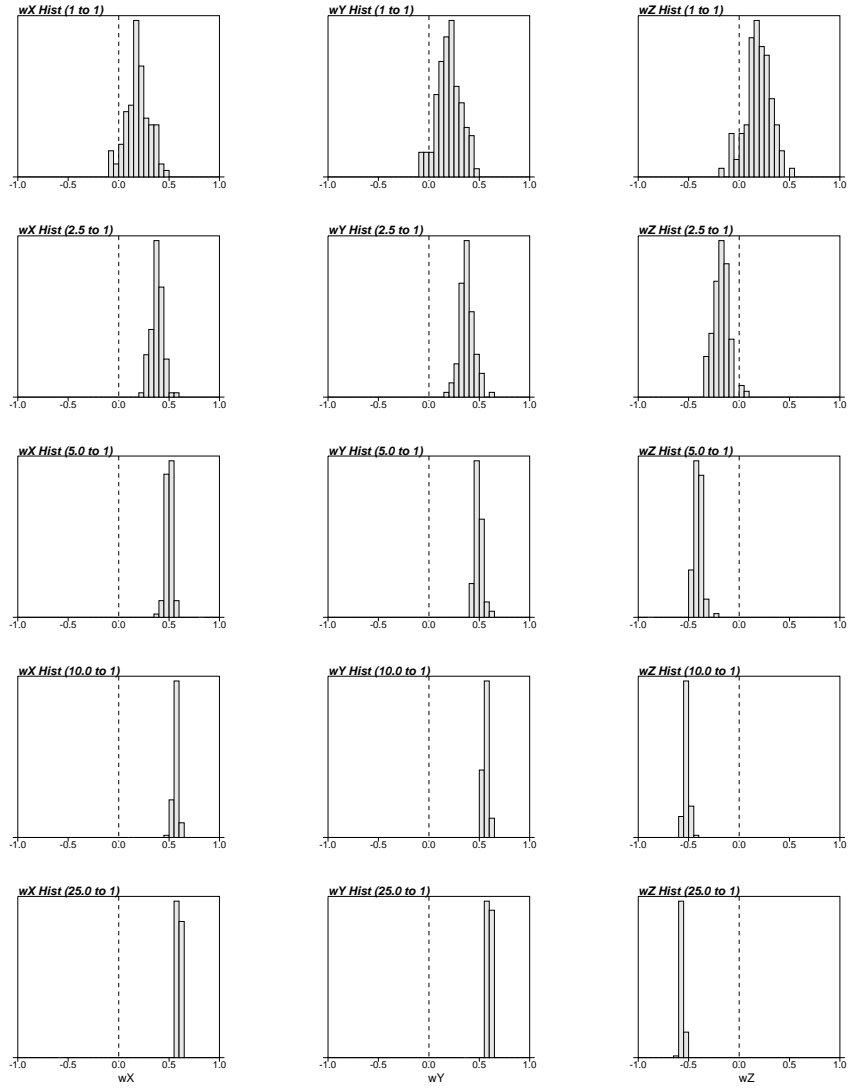


Figure 4: The effects of changing the anisotropy ratio in sgsm: histograms of ω_X , ω_Y , and ω_Z .

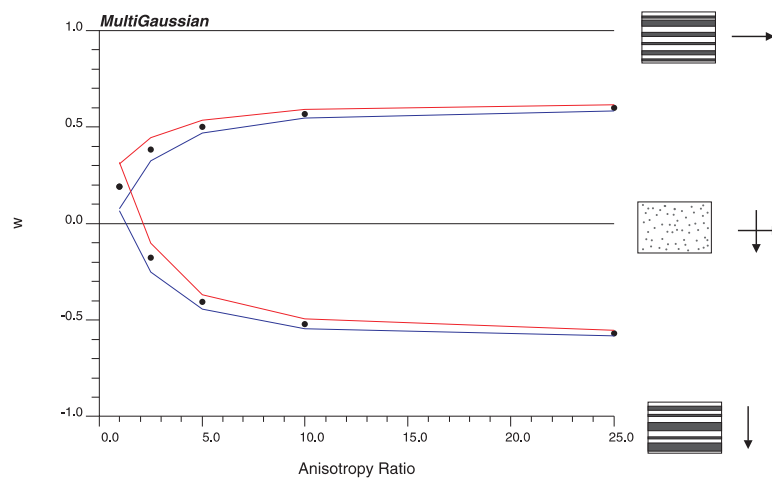


Figure 5: The effect of the anisotropy ratio on ω when using sgsim. The black dots are the mean ω values for all three primary direction; increasing ω for X and y, and decreasing ω for Z. The red line is one standard deviation above the mean the blue line is one standard deviation below the mean.

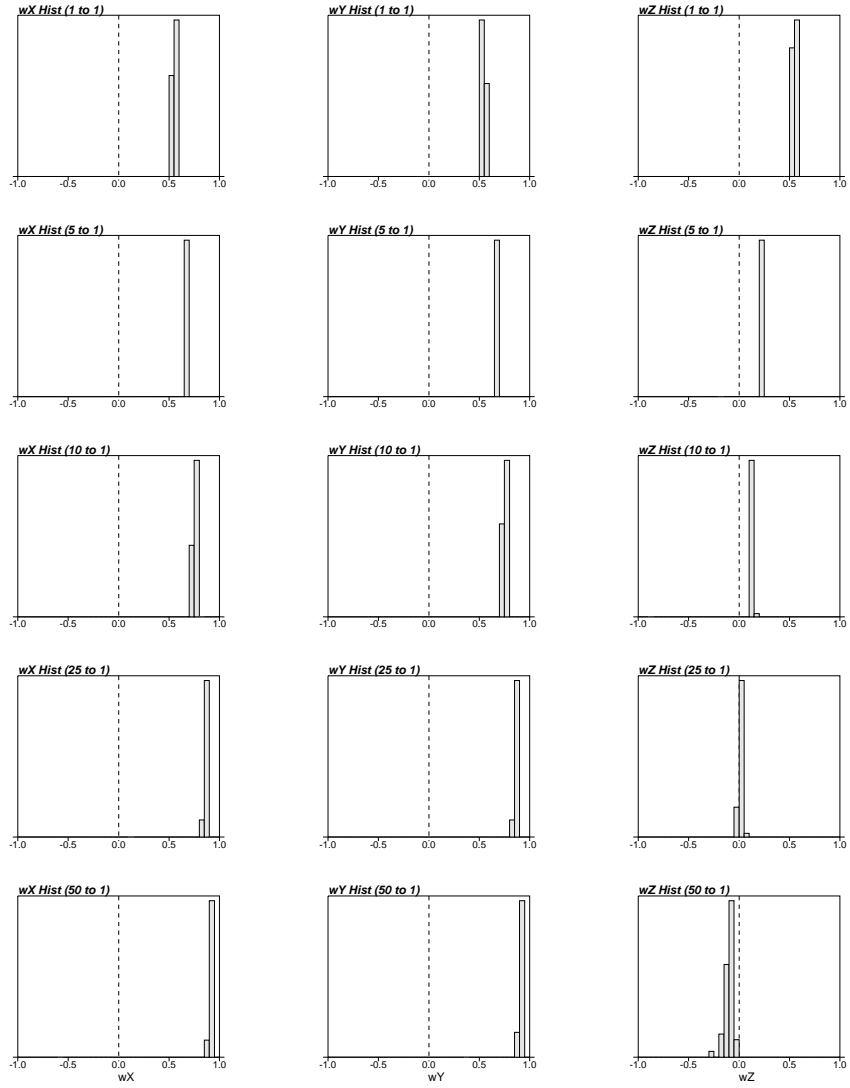


Figure 6: The effects of changing the anisotropy ratio in ellipsoid when looking at the histograms of ω_X , ω_Y , and ω_Z .

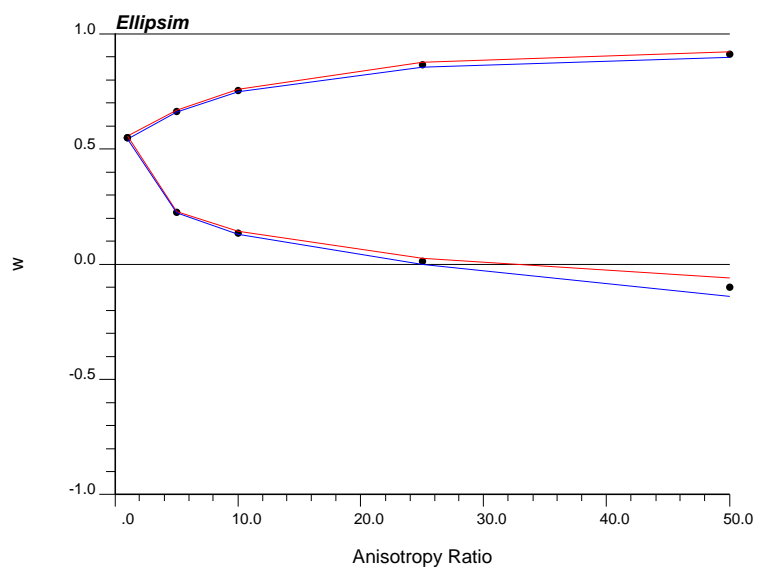


Figure 7: The effect of the anisotropy ratio on the ω using ellipsim. The top lines represent the X and Y directions and the bottom lines represent the Z direction.

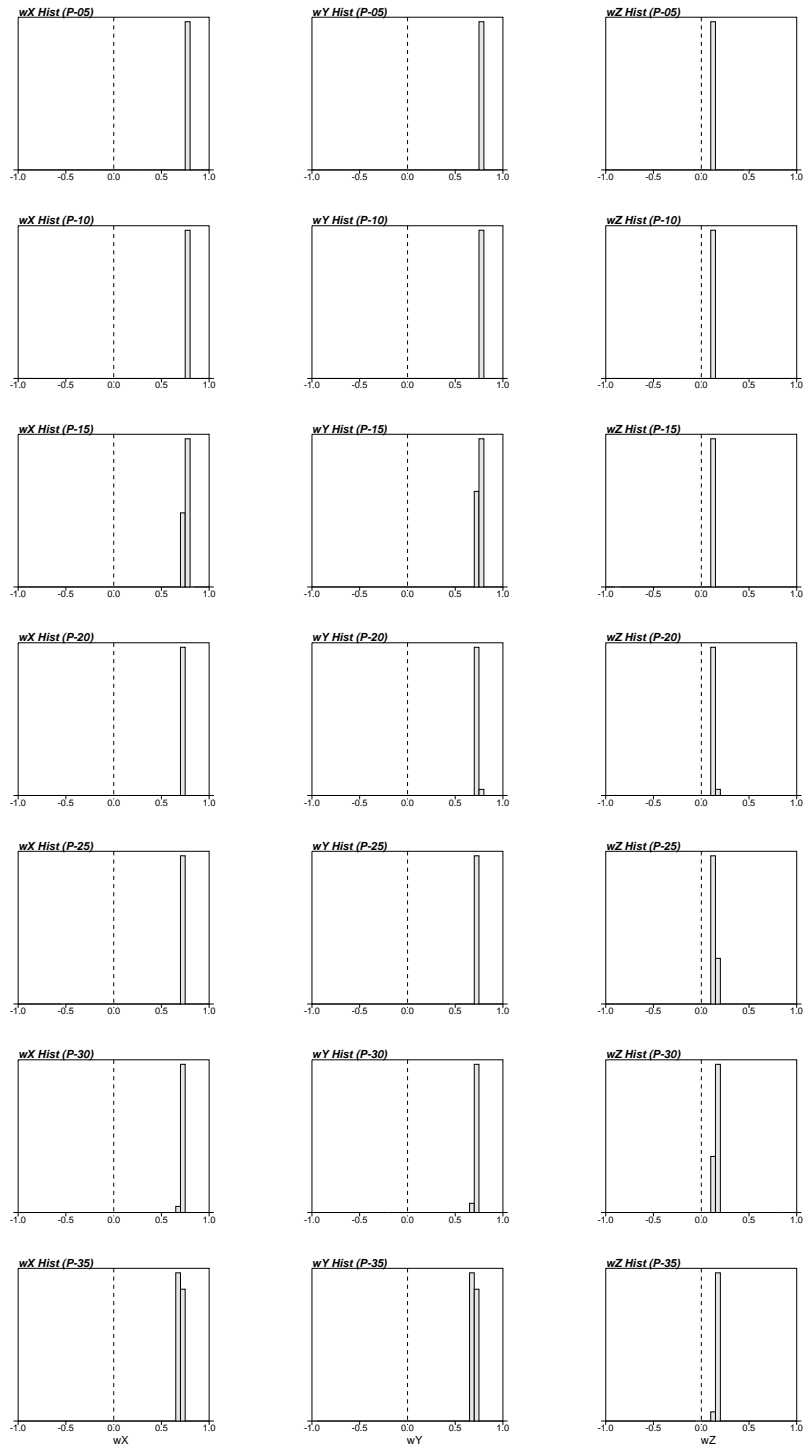


Figure 8: The effects of changing the sandstone percentage from 5% to 35% in ellipsoid when using a base case anisotropy ratio of 10 to 1.

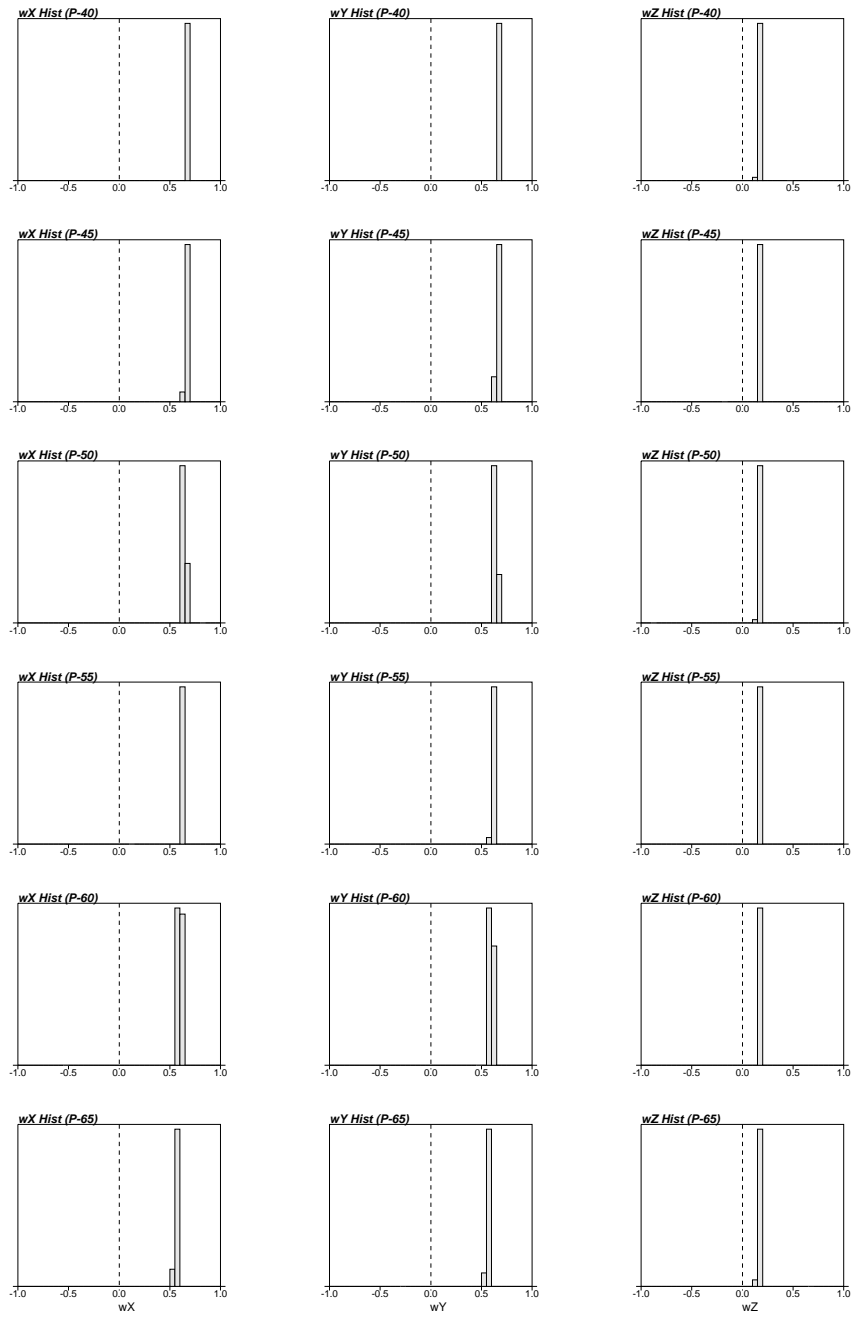


Figure 9: The effects of changing the sandstone percentage from 40% to 65% in ellipsim when using a base case anisotropy ratio of 10 to 1.

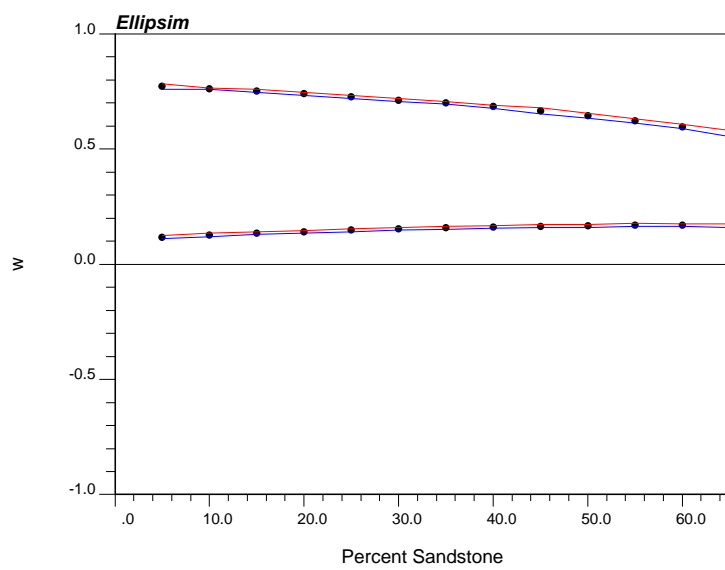


Figure 10: The effect of the percentage of sandstone on the calculated ω using ellipsim. The top lines represent the X and Y directions and the bottom lines represent the Z direction.

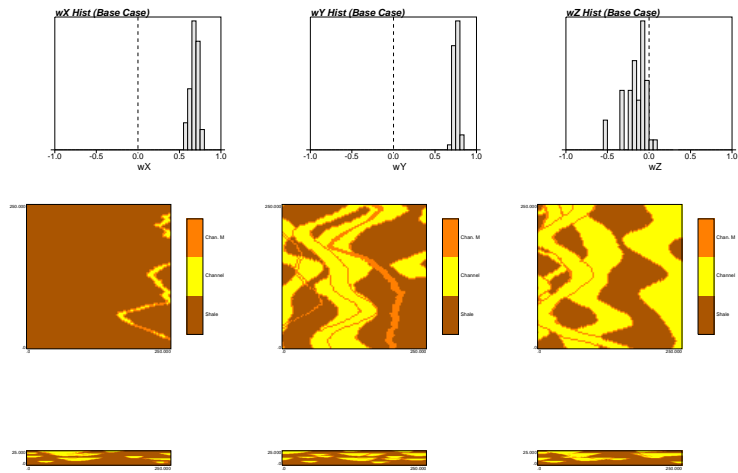


Figure 11: The 3 histograms for ω_X , ω_Y , and ω_Z for the base case of fluvsim.

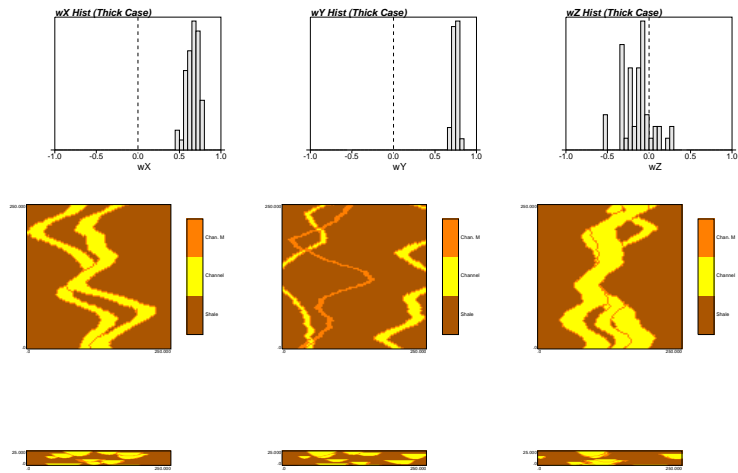


Figure 12: The 3 histograms for ω_X , ω_Y , and ω_Z for the “thick” case of fluvsim.

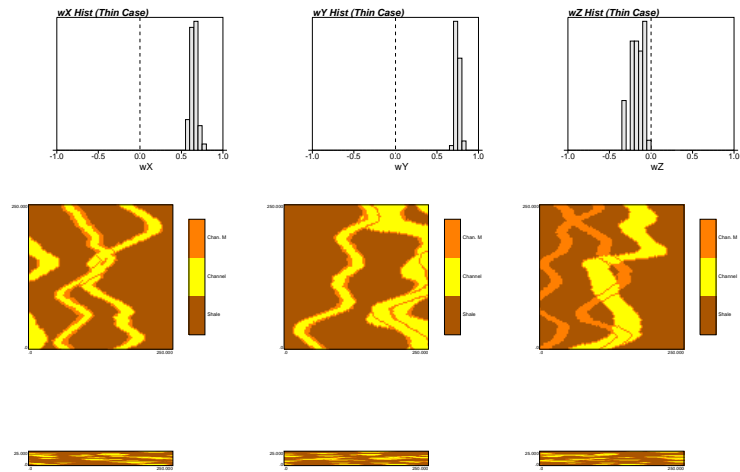


Figure 13: The 3 histograms for ω_X , ω_Y , and ω_Z for the "thin" case of fluvsim.

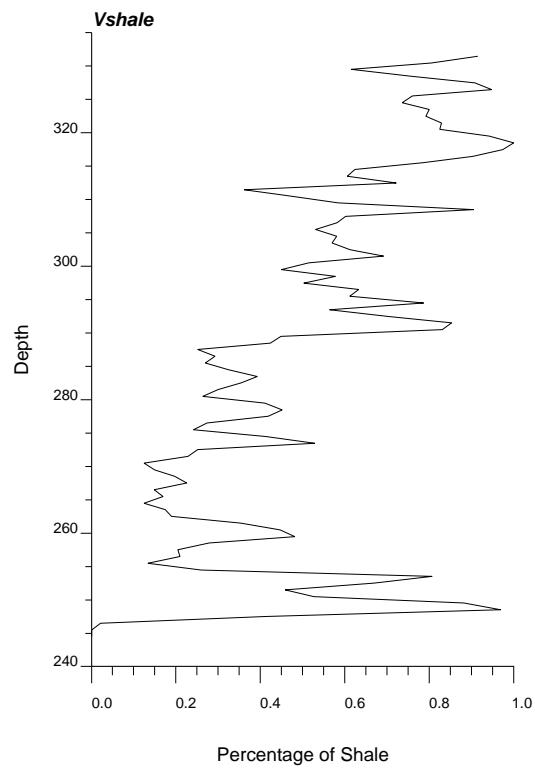


Figure 14: Plot of V_{shale} log data with depth.

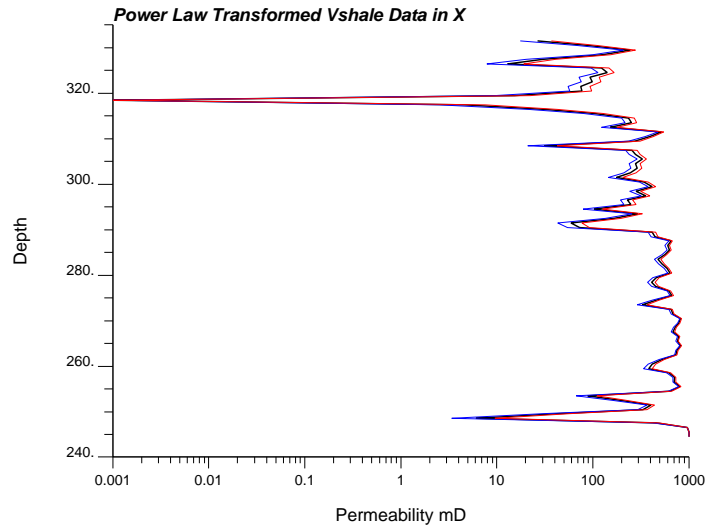


Figure 15: Plot of the power law transformed Vshale data to permeability (mD) in the X direction. The thick black line is the mean of ω , the outer light lines correspond to the P_{10} , blue, and P_{90} , red, values for ω .

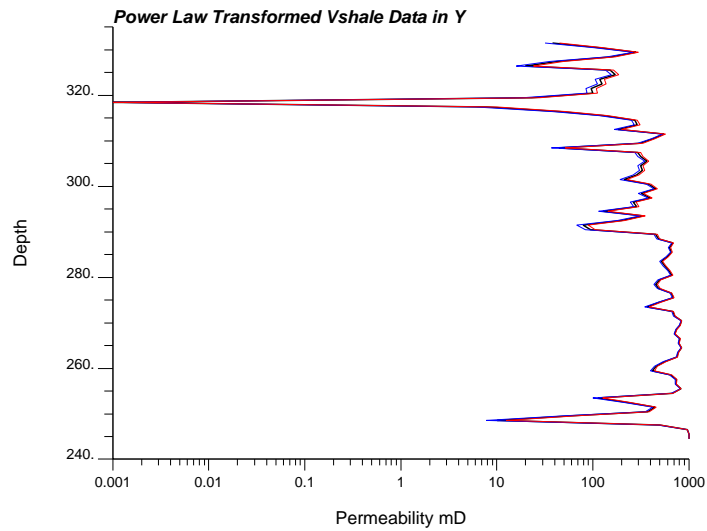


Figure 16: Plot of the power law transformed Vshale data to permeability (mD) in the Y direction. The thick black line is the mean of ω , the outer light lines correspond to the P_{10} , blue, and P_{90} , red, values for ω .

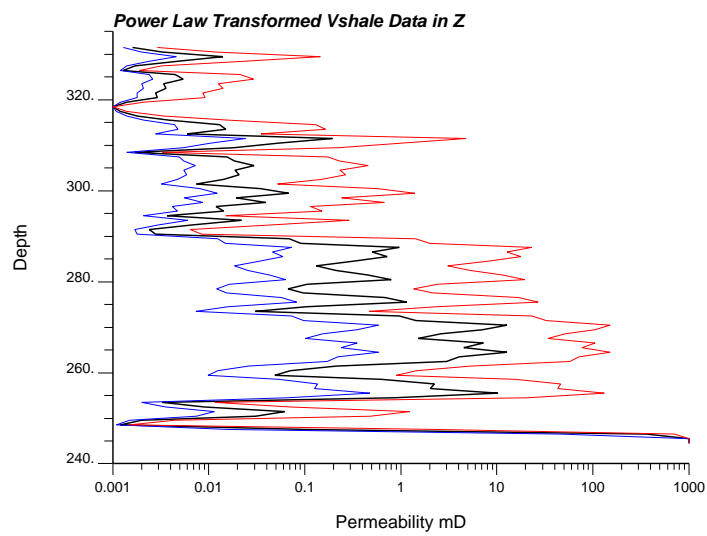


Figure 17: Plot of the power law transformed Vshale data to permeability (mD) in the Z direction. The thick black line is the mean of ω , the outer light lines correspond to the P_{10} , blue, and P_{90} , red, values for ω .

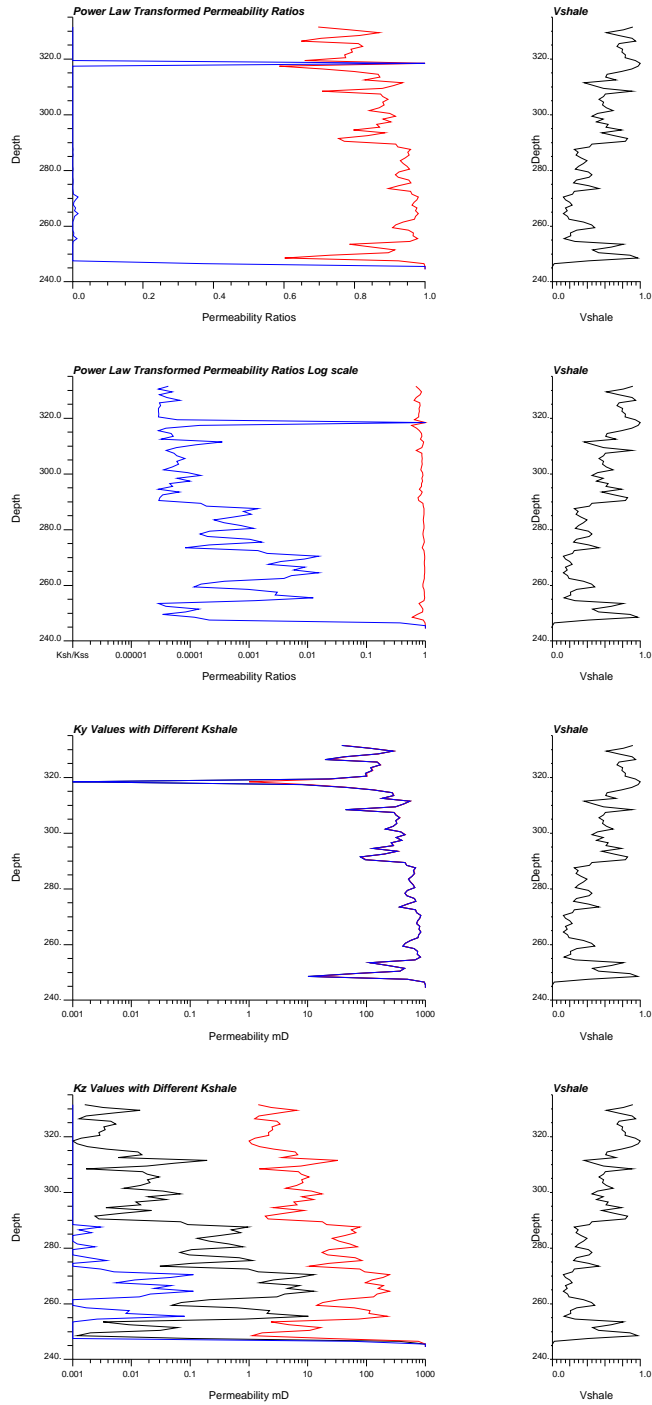


Figure 18: The upper two plots show k_x/k_y ratios (red) and k_z/k_y ratios (blue) in arithmetic and log scales. The last two plots show the same ratios with different values for K_{shale} . The red line is $K_{sh} = 1.0$, the black line is $k_{sh} = 0.001$, and the blue line is $k_{sh} = 0.000001$.

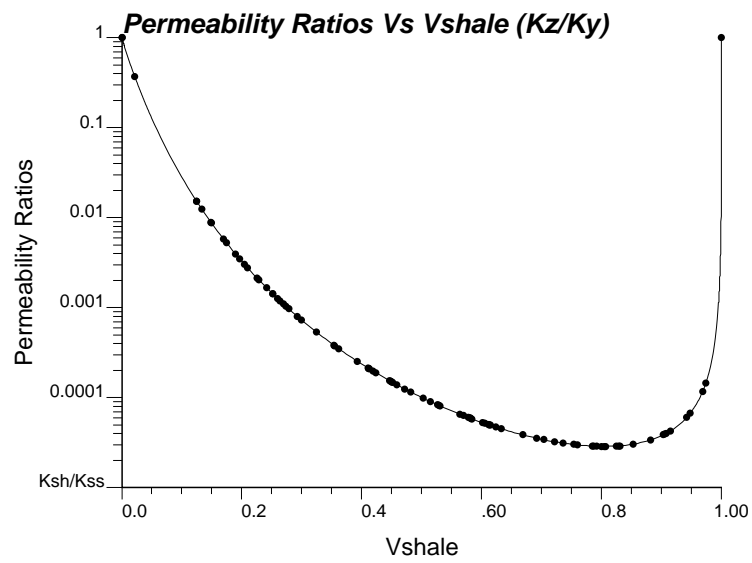
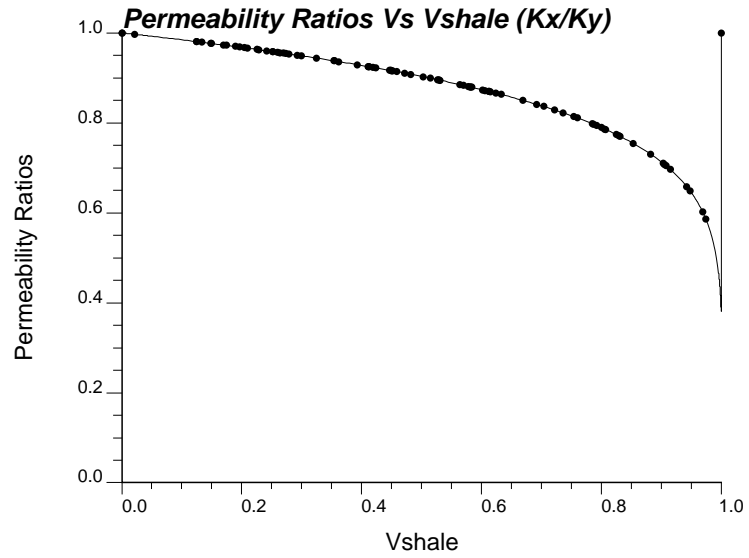


Figure 19: The top graph shows how the k_x/k_y permeability ratio changes with V_{shale} . The solid line is the theoretical results, which is reproduced perfectly by the calculated values, shown in dots. The bottom graph shows the k_z/k_y ratios on a log scale. The theoretical lower limit is given by k_{sh}/k_{ss} .

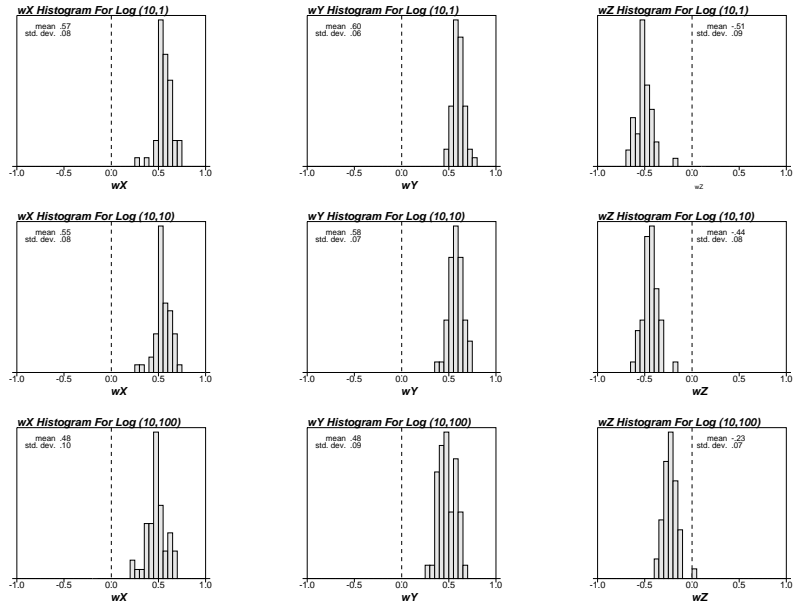


Figure 20: The histograms of ω for lognormal transforms with a mean of 10 and standard deviations of 1, 10, and 100.

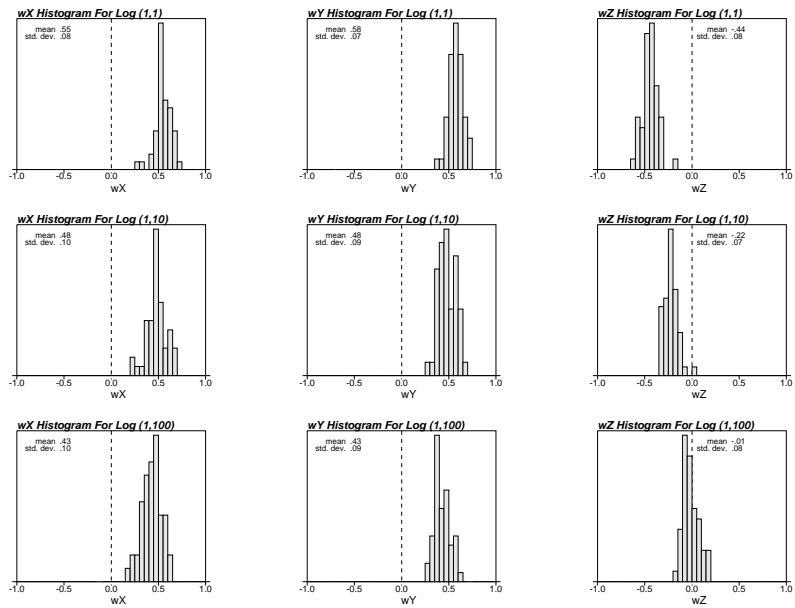


Figure 21: The histograms of ω for lognormal transforms with a mean of 1 and standard deviations of 1, 10, and 100.

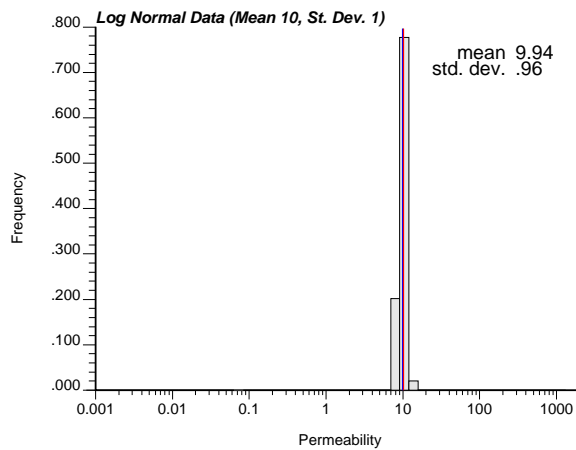
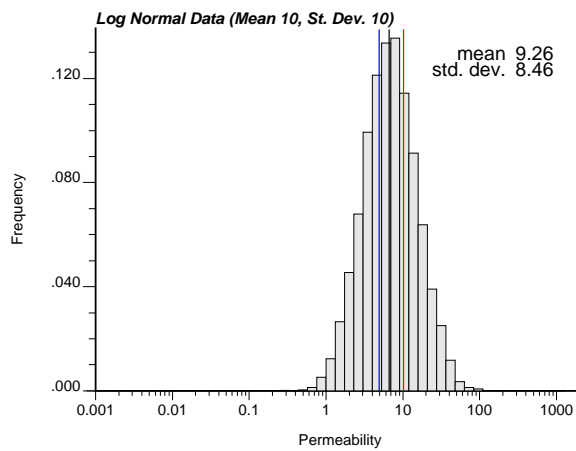
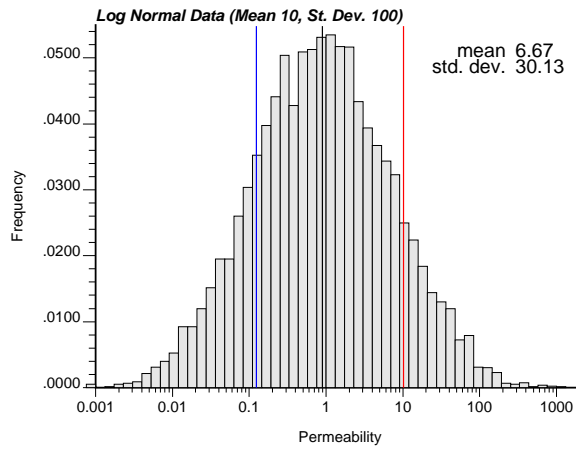


Figure 22: The histograms of the lognormal data with a mean of 10 and standard deviations of 100, 10, and 1 respectively from top down. The three vertical lines show the harmonic (blue), geometric (black), and arithmetic (red) permeabilities.